Slender Pillar Stability Analysis in Open Stope Mining

Pedro Samuel Soares Teopisto

Instituto Superior Técnico, Lisboa, Portugal

October 2019

Abstract

The increasing demand in production, linked to a greater concern in terms of geotechnical stability and safety, implies challenging and constant adaptations of the mining methods by the mining industry. Bearing that in mind, the main focus of this thesis is to analyse the stability of pillars that remain between stopes which are 15m large and 40m tall, in Lombador deposit, Neves Corvo Mine.

For that matter, a tridimensional numerical modelling software (RS3, from Rocscience), was used, in particular using the finite element method, in order to evaluate the stability of two different scenarios comprising the use of the modelling sequence proposed by Somincor, in which the first scenario corresponds to pillars with 20m in height while the second scenario comprises pillars with 40m in height.

The analysis of the parameters used to study the pillar stability (maximum principal stress, minimum principal stress, total displacements and factor of safety) dictated that the scenario in which the pillars have a lower height were generally more stable.

Keywords: Underground mining, Pillar Stability, Numerical Modelling, Finite Element Method.

1. Introduction

Despite its little size when compared to other countries that dominate the geological resources exploitation worldwide, Portugal is very rich in terms of geological diversity and has a high potential in mineral resources.

The increasing demand in production, linked to a greater concern in terms of geotechnical stability and safety, implies challenging and constant adaptations of the mining methods by the mining industry.

As of this, the scope of this work is to perform a pillar stability analysis regarding two different scenarios: the first, which comprises pillars 15m wide by 20m tall, the second comprising pillars 15m wide by 40m tall. Following the modelling sequence proposed by Somincor, it is desirable to establish an optimal balance between the chosen mining method and safety.

2. State of the art

Regarding the Mining Engineering field, pillars can be seen as structures with capital importance that play a critical role in the stability of underground excavations. They are frequently present in any type of underground mines, them being permanent or temporary. While permanent pillars are required to fulfil their function throughout the entire mine life, temporary pillars are usually removed as the exploration advances.

Salamon (1983) describes three different types of pillars, according to their function: support pillars, protection pillars and control pillars. Additionally, Potvin (1985) classifies pillars in four distinct groups: plate pillars, separation pillars, stub pillars and inclined pillars.

Regarding the pillar design methods, the most and simplest approach is based on the condition that, whenever the stress on a given pillar exceeds its strength, the pillar fails. This statement forms the concept of Safety Factor, which can be defined by Equation 1:

$$S.F. = \frac{Pillar\ Strength}{Stress\ acting\ on\ pillar} \quad (1)$$

The safety factor can be regarded as an important stability analysis tool. Nevertheless, the Stress acting on a pillar and its Strength must be correctly estimated. Potvin, Hudyma and Miller, (1989) identified the critical (or significant) variables that play a large role in the pillar strength. These variables are:

- Uniaxial Compressive Strength of the rock;
- Load acting on the pillar;
- Pillar geometry;
- Geological features (joints, fractures, etc);
- Pillar volume;
- Effect of backfill;
- Effect of explosives;

In terms of pillar design methods, one can identify three main methods:

- Theoretical/analytical methods – these methods rely on mathematical concepts and formulations to describe the rock mass behaviour and its influence in pillar stability. These are challenging and unpredictable methods, given the variability of the rock mass conditions (Lunder, 1994); One of the most well-known theoretical methods is the tributary area method, introduced by Bunting in 1911.
- Empirical methods – these methods rely on experience acquired during the application of successful case studies and are the most accepted and used worldwide. Numerous authors have developed empirical methods throughout the last couple decades, namely the methods developed by Salamon and Munro (1967), Obert and Duvall (1967), Hedley and Grant (1972) and Lunder and Pakalnis (1997).
- Numerical methods – these methods are based on mathematical algorithms capable of solving complex problems. They are experiencing an increase in demand, as new and more sophisticated tools are starting to be available to the common user. There are four main types of Numerical methods: Finite Elements, Finite Differences, Boundary Elements and Discrete Elements. In the scope of this study, the Finite Elements Method was used.

Regarding the Finite Element Method, it is particularly useful in analysing the state of stress, when dealing with complex mining geometries, and estimating the rock mass deformational parameters, such as total displacements (Sepehri, Apel e Szymanski, 2013). In this method, the domain of the problem is approached as a series of several sub-problems (which we call elements) connected at each other in specific locations, the nodes, as exemplified in Figure 1.

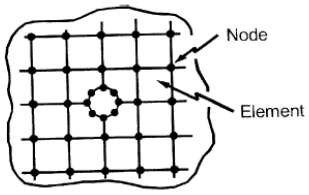

Figure 1: Schematical representation of the finite element method (Singh, Singh & Murthy, 2010).

Regarding pillar failure mechanisms, Hudyma (1998) described two ways in which this failure can occur: progressive failure and violent failure.

On the one hand, progressive failure generally occurs in a long period of time, characterised by a gradual and slow release of the energy stored in the pillar. On the other hand, violent failure corresponds to a sudden release of energy, which can cause severe personal, material or even environmental damage (Lunder, 1994).

3. Case study – description and methodology

3.1. Neves Corvo Mine

Neves Corvo mine is located in the Alentejo region, roughly 220km southeast of Lisbon, being part of the Beja district. Neves Corvo is owned and operated by Somincor, a subsidiary of Lundin Mining.

In terms of geology, the mine comprises seven different orebodies, which are designated as volcanogenic massive sulphides, occurring as polymetallic lenses with mainly copper and zinc. These orebodies all belong to the Iberian Pyrite Belt, where we can identify three main units (Carvalho e Ferreira, 1993): the Volcano-Sedimentary Complex (VSC), the Phyllite Quartzite Group (PQG) and the Flysch formation.

3.2. Numerical Models – methodology

The information required for this analysis was either provided by the company or obtained in the field. The values presented in Table 1 refer to the geomechanical properties of the materials used in the models.

Table 1: Geomechanical properties of the materials considered in the models (Somincor, 2019).

Propriedade \ Material	Xistos	Sulfuretos Maciços	Pasta (5% de cimento)
Peso volúmico, γ (MN/m³)	0.029	0.044	0.0215
Módulo de *Young*, *E* (MPa)	30 000	87 500	500
Coeficiente de Poisson, υ	0.32	0.14	0.25
Resistência à compressão uniaxial, σ_c (MPa)	50	250	0.5
Resistência à tração, σ_t (MPa)	0.28	2.10	0.06
Ângulo de atrito, ϕ (º)	41.5	59.3	42.0
Coesão, c (MPa)	1.80	7.12	0.11

In terms of the state of stress admitted in the models, the Table 2 presents the values used, expressed as stress gradients.

Table 2: Gradient of the state of stress considered in the models.

	Gradiente de tensão (MPa/m)	*Mergulho (º)*	*Direção de Mergulho (º)*
σ_1	0.083	20	132
σ_2	0.039	30	30
σ_3	0.025	53	250

In terms of the models created with the RS3 software, 4 models were produced: 2 models within one single lithology (massive sulphides) and 2 models with the presence of a hanging wall geological contact (black shales/massive sulphides). In each one of these pairs, one model corresponds to 20m high pillars and the other one to 40m high pillars. The figure 2 clarifies the difference between the model with and without the contact.

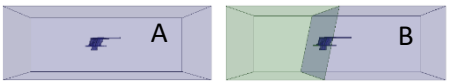

Figure 2: Model without (A) and with contact (B), for the case of the 40m high pillars.

Based on the mining sequence proposed by Somincor, a 3D geometry was built in Rhinoceros 3D® (Figure 3), which was then introduced in the RS3 software.

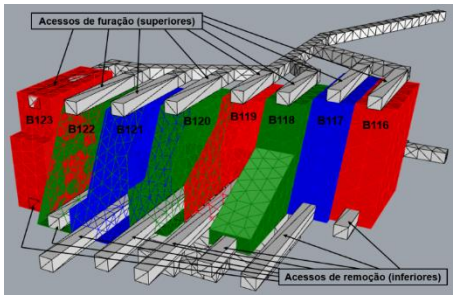

Figure 3: Perspective view of the created geometry in Rhinoceros 3D®.

All the models were created in order to try to faithfully represent the reality, although in a simplistic manner. The aim is to study the state of stress redistribution on different pillars caused by the excavation of the stopes, in a staged manner.

After introducing the geometry in the software, the next step is to create an external boundary of the model, which the represents the extents of the analysis. Figure 4 represents the external box created, with an Expansion factor of 3, which means the external box is 3 times bigger than the geometry itself.

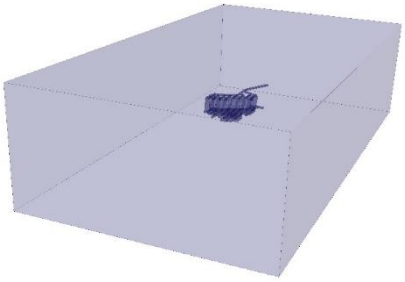

Figure 4: External box creation.

Next, based on the state of stress given Table 2, we calculate the state of stress at our desired depth. The model is 530m below surface, corresponding to the state of stress given as in Figure 5.

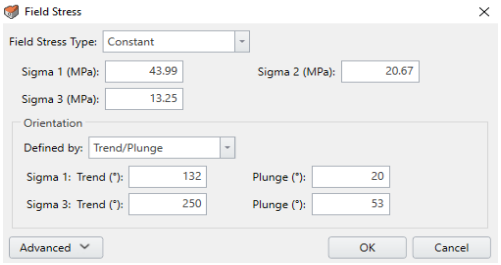

Figure 5: State of stress considered for a depth of 530m.

After properly defining the state of stress, one must then introduce the geomechanical properties of all materials considered in the models. After that, it is time to create the finite element mesh of the whole model and define the restraints, which represents in which direction the model is allowed to move. After these steps, we obtain the final model, ready to compute (Figure 6).

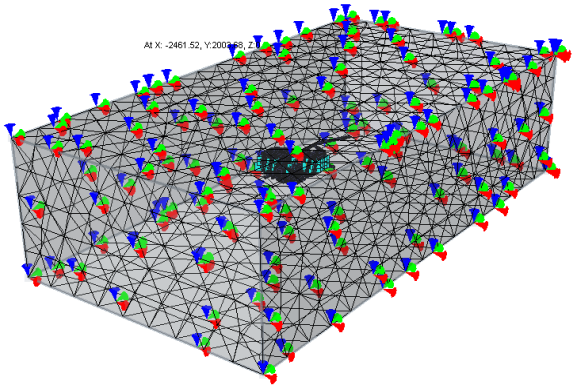

Figure 6: Mesh application and restraints definition.

After computing the results of all models, 6 pillars were chosen to analyse, in terms of state of stress characterization and deformation. Four parameters were studied: Maximum principal stress σ_1, minimum principal stress σ_3 , total displacements and safety factor.

For a quantitative analysis, 9 points were chosen within the pillar in order to measure the values of the parameters referred above. The points were distributed as groups of 3, disposed at 3 different pillar heights, as shown in Figure 7.

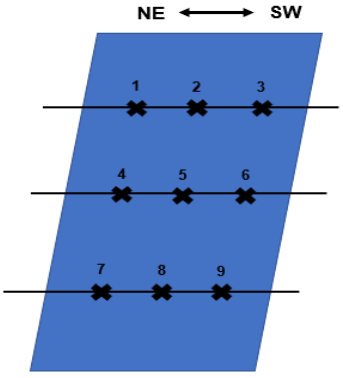

Figure 7 – Distribution of the 9 points for the quantitative analysis.

The pillars in this study were divided into 4 categories:

1. Abutments pillars (EB123 and EB116) (Figure 8);

2. Primary Sequence pillars (B119 and B121) (Figure 9);

3. Secondary Sequence pillar (B117) (Figure 10);

4. Tertiary Sequence pillar (B120) (Figure 11).

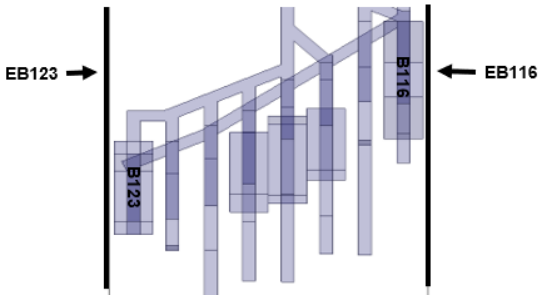

Figure 8: Location of the abutment pillars (marked in black).

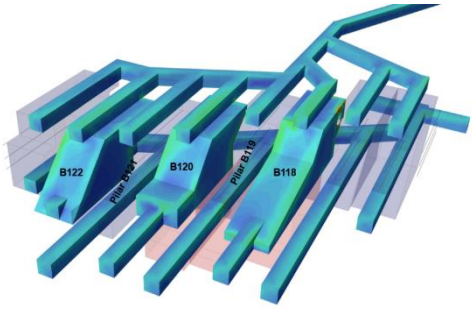

Figure 9: Location of the primary pillars.

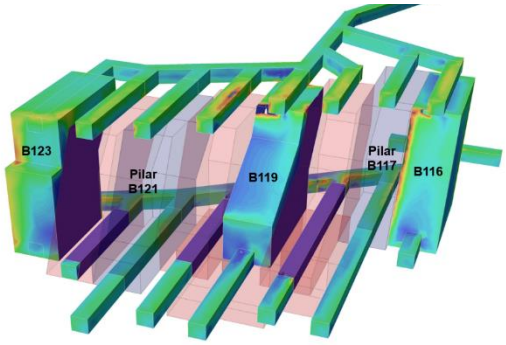

Figure 10: Location of the secondary pillar.

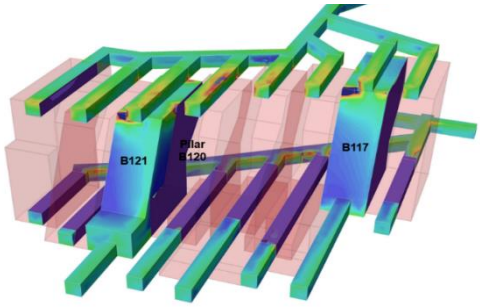

Figure 11: Location of the Tertiary pillar.

4. Results and Discussion

The results from the computed models are presented here. In the impossibility of presenting all the results, the Safety Factor was chosen to illustrate the results obtained in the models, as it is the most significant parameter in the analysis. However, in the B120 pillar, the total displacements will be analysed instead of the safety factor, as it is more relevant for the study of that pillar in particular.

The results are divided in the categories presented in the last chapter.

4.1. EB123 Pillar – Safety Factor

The variation of the Safety Factor along the stages is present in Figure 12.

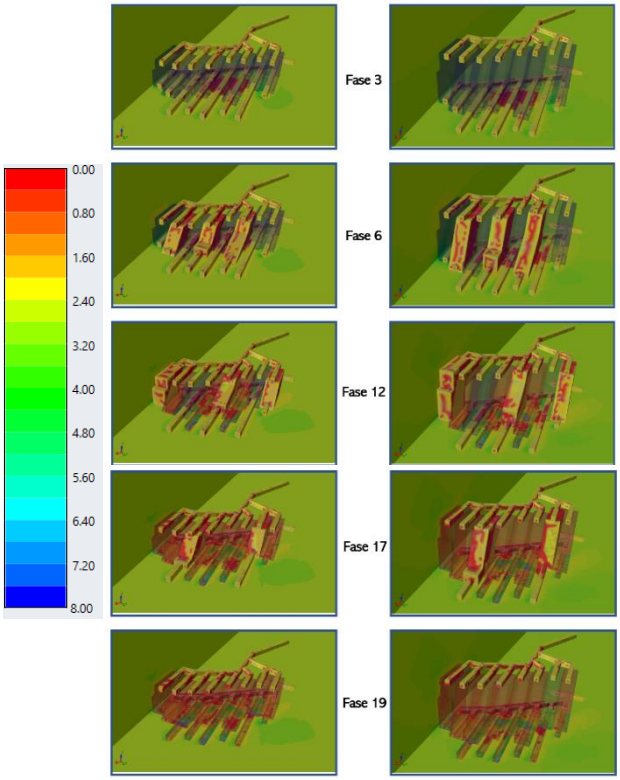

Figure 12 – Safety Factor Variation in pillar EB123.

As we can see from figure 12, the safety factor is around 2 and 3 in stages 3 and 6, in both scenarios. However, in stage 12, the safety factor decreases in the center of the pillar, with greater expression in the 40m scenario (right).

In terms of stability, the safety factor never goes below the unity, which denotes no stability problems, except for a small region in the upper region of the pillar, in the 40m scenario.

4.2. EB116 Pillar – Safety Factor

The variation of the Safety Factor along the stages, in pillar EB116 is present in Figure 13.

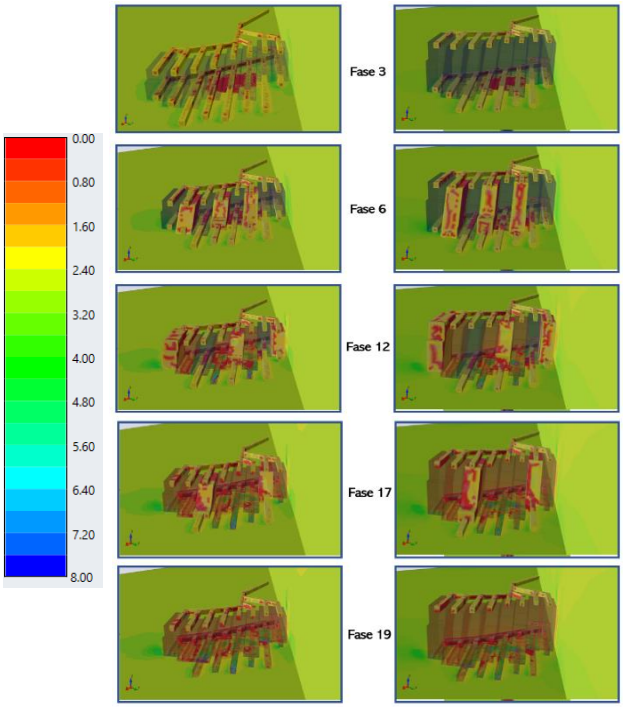

Figure 13 – Safety Factor Variation in pillar EB116.

As we can see from stage 3, the safety factor inside the pillar ranges from 2 to 4. After stage 6, the safety factor does vary too much, except for a small region whose safety factor drops from 3 to 2. After stage 12, the safety factor in the entire region of the pillar decreases from around 3 to around 1.6. In the 40m scenario, the safety factor decreases a bit more than in the 20m scenario.

4.3. B119 Pillar - Safety Factor

The variation of the Safety Factor along the stages, in pillar B119 is present in Figure 14.

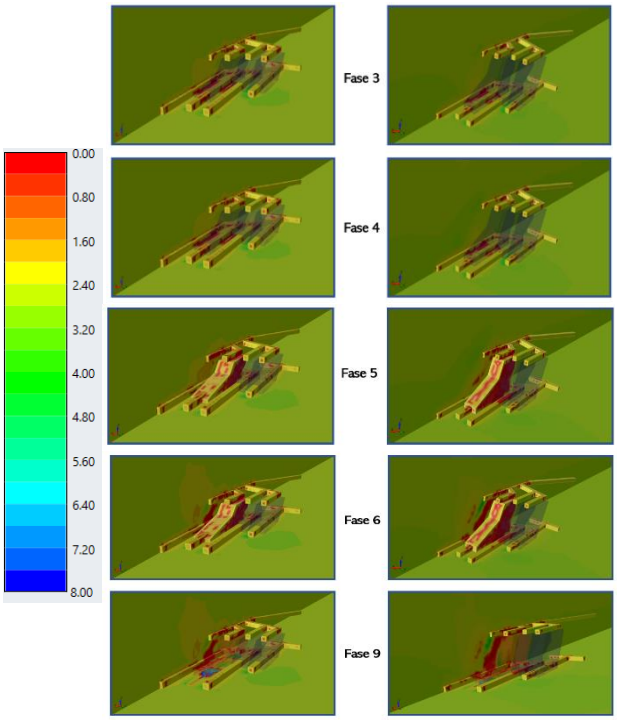

Figure 14 – Safety Factor Variation in pillar B119.

Right after stage 3, there are some regions in the roof of both accesses with safety factors below 1, which denotes instability.

As the exploration goes on, the safety factor inside the pillar decreases from 2.4 (stage 3) to 1.6 (stage 5). In stage 6, there is a significant reduction of the safety factor in the center of the pillar, reaching values below 1.

4.4. B121 Pillar - Safety Factor

The variation of the Safety Factor along the stages, in pillar B119 is present in Figure 15.

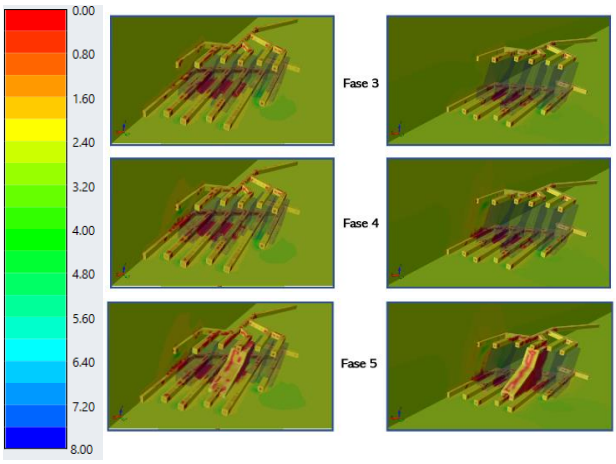

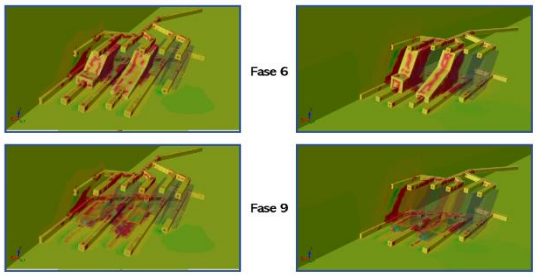

Figure 15 – Safety Factor Variation in pillar B121.

Similarly to pillar B119, right after stage 3, there are some regions in the roof of both accesses with safety factors below 1, which denotes instability. This is true for both scenarios. After stage 6, the instability regions propagate from the roof of the accesses to the interior of the pillar, with safety factors dropping below 1 along the entire pillar. These phenomena is much more significative in the 40m scenario.

4.5. B117 Pillar - Safety Factor

The variation of the Safety Factor along the stages, in pillar B117 is present in Figure 16.

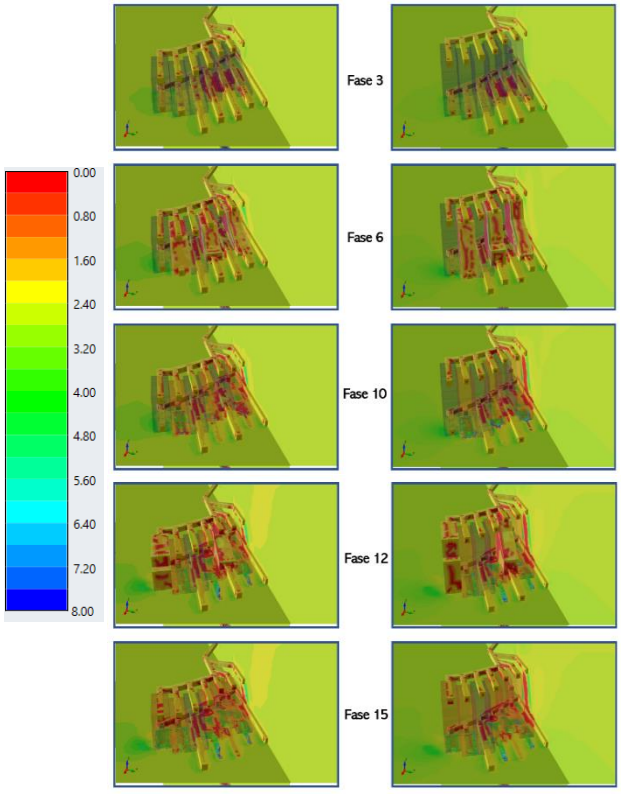

Figure 16 – Safety Factor Variation in pillar B117.

After stage 3, there are some instability regions in the lower accesses in both scenarios, although it is a bit more significant in the 20m scenario. At stage 10, the instability propagates to the interior of the pillar, much more significant for the 40m scenario. At stages 12 and 15, the instability practically doesn't change, compared to stage 12.

4.6. B120 Pillar - Total Displacements

The variation of the Total Displacement along the stages, in pillar B120 is present in Figure 17.

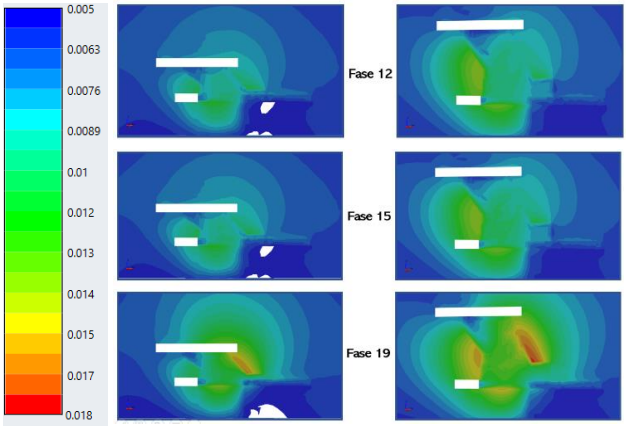

Figure 17 – Total Displacement Variation in pillar B120.

In stage 12, when the pillar is surrounded by a rock pillar and an open stope, the displacements are greater in the "left side" of the pillar, being much more significative in the 40m scenario.

In stage 15, when the pillar is surrounded by a rock pillar and a pastefill pillar, the changes are practically unrecognizable.

In stage 19, when the pillar is surrounded by two pastefill pillars, the displacements rise up, especially in the "right "side" of the pillar, being much more representative in the 40m scenario.

4.7. Influence of the lithological contact

After analysing all the parameters in all models, the results were very similar.

Nevertheless, some differences were observed, not what concerns the stress redistribution and deformation in the pillars themselves, but in the accesses. In the figure 18 it is represented the difference (in the pillar B119) between the model 2 (left, without contact) and the model 4 (right, with contact).

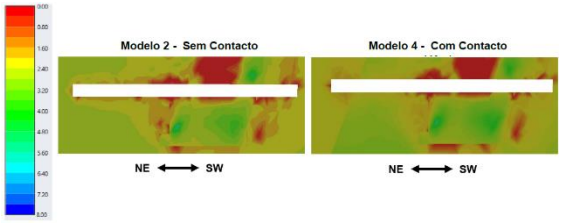

Figure 18: Safety factor for the model without contact (left) and for the model with contact (right).

As one can observe, the safety factor is very similar inside the pillar. In the lower access, however, there is more instability in that accesses' roof, in the model with contact.

Additionally, since the final part of the lower access is excavated in black shales, the instability is higher in that region, when compared to the access in the model without contact, which is entirely excavated in massive sulphides.

5. Conclusions

In what concerns the safety factor, it was observed some regions of instability right after escavating the accesses in stage 3, in the most rock pillars observed. As the sequence progressed, the instability generally propagated to the interior of the pillar, being the pillar B119 and B121 the most critical in terms of area of influence of the said instability. Relatively to the abutment pillars, there were no major signs of instability, where the safety factors were always above 1, except for a little region in the top of the EB123 pillar. Relatively to the pastefill pillar, there were no major differences between stages 12 and 15. However, when the sequence progressed to the stage 19, the displacements rose up in some areas of the pillar (and around it, too). This difference can be attributed to the fact that the rock has a Young's Modulus that is 175 times higher than the pastefill Young's Modulus, which is why, when the pastefill pillar is between two other pastefill pillars, it can deform easier. On what concerns the lithological contact, there were no significant differences between the results observed pillar wise. However, the accesses on the model with contact tend to be a little more unstable, especially in the final part of the lower access.

6. References

- Carvalho, P., & Ferreira, A. (1993). Geologia de Neves Corvo: Estado Actual do Conhecimento. Castro Verde: Somincor.
- Hudyma, M. (1988). Development of Empirical Rib Pillar Design Criterion for Open Stope Mining – Thesis to obtain the degree of Master of Applied Science. Department of Mining and Mineral Process Engineering, University of British Columbia, British Columbia, Canada.
- Lunder, P. J. (1994). Hard Rock Pillar Strength Estimation – An Applied Empirical Approach - Thesis to obtain the degree of Master of Applied Science. Department of Mining and Mineral Process Engineering, University of British Columbia, British Columbia, Canada.

- Potvin, Y. (1985). Investigation of Underground Mine Pillar Design Procedures - Thesis to obtain the degree of Master of Applied Science. Department of Mining and Mineral Process Engineering, University of British Columbia, British Columbia, Canada.
- Potvin, Y., Hudyma, M., & Miller, H. D. (1989). Rib Pillar Design in Open Stope Mining. Bull Canadian Institute of Mining and Metallurgy, vol.82, pp.31-36.
- Salamon, M. D. (1983). Role of Pillars in Mining. In Rock Mechanics in Mining Practice, Budavari (ed.), Johannesburg, pp.173-200.
- Sepehri, M., Apel, D. B. & Szymanski, J. (2013). Full Three-Dimensional Finite Element Analysis of the Stress Redistribution in Mine Structural Pillar. J Powder Metallurgy and Mining, 3: 119. doi: 10.4172/2168-9806.1000119.
- Singh, G. S., Singh, U. & Murthy, V. M. (2010). Applications of Numerical Modelling for Strata Control in Mines. Geotechnical and Geological Engineering, vol.28, pp.513-524.